Renewable Energy, Environment, and Power Quality Journal (REE&PQJ)
ISSN:3020-531X
Volume 24, January 2026

A Modular Multi-Technology Generator Model for EMT Stability Studies in Power Systems with Large Amounts of Converter-based Generation

Jesús Castro Martínez[1], Santiago Arnaltes[1], José Luis Rodríguez[1], Javier Renedo[2], Edgar Nuño Martínez[2], Macarena Martín Almenta[2], Sergio Martínez Villanueva[2]

[1] Department of Electrical Engineering, Carlos III University of Madrid. 28911 Leganés, Madrid (Spain)

[2] Red Eléctrica – Redeia. 28109 Alcobendas, Madrid (Spain).

Abstract. This paper explores the integration of converter-based generation (CBG) into power systems, analyzing their impact on power system stability. For this purpose, a simulation tool consisting of comprehensive, aggregated models integrating several generation technologies into a power system for dynamic simulation has been developed to represent three prominent generation technologies: synchronous generation (SG), grid-following converters (GFL), and grid-forming converters (GFM). The proposed modular multi-technology generator model allows to set the penetration level of each technology at any bus of the system, thus facilitating stability assessment of power systems with large amounts of CBG. Electromagnetic-type (EMT) studies are carried out in a small test system to analyse the impact of the GFL/GFM generation ratio on power system stability. The results show the capability of the proposed tool for testing the impact of the generation mix in the stability of the system, highlighting the importance of GFM generation to operate in with low amounts or in absence of synchronous generators in the system.

Key words. EMT simulation, grid-forming converters, power system stability, renewable energy.

1. Introduction

During the last decade, the evidence of climate change and the uncertainties regarding the prices of fossil fuels have motivated the development and spread of renewable generation technologies (RGT) in advanced power systems [1]. As many of these RGT should not be directly connected to the grid, they usually take advantage of the capabilities of power electronics. However, as converter-based generation (CBG) is expanding, conventional generation, based on synchronous generators (SG) is being replaced. This implies some inconveniences for power grids such as the reduction of physical inertia and grid strength in the power system [2], capabilities that were traditionally provided by conventional synchronous generators.

Several control techniques have been proposed in order to make CBG fit for conventional power systems [3], [4]. In this paper, the two main control strategies for CBG are analysed: grid-following (GFL) and grid-forming (GFM) converters [5].

The basis of GFL control strategies is to make the converter behave as a current source [6]. In this strategy, the synchronization to the grid is achieved by means of a Phase-Locked Loop (PLL), which is unsensitive to grid disturbances [7]. Therefore, GFLs need an existing grid with a certain strength for stable operation and stand-alone operation is not possible. Nevertheless, are able to provide some grid support with external measurements (called grid-supporting converters by some authors [8]). Applied to the frequency control, one of the most widespread approaches is synthetic inertia control and frequency control [3]. However, external measurements and filtering add some response delay, which may affect system stability when the penetration of this technology in the system is high [9].

A different approach is GFM control. The goal of this strategy is to make the power converter behave as a voltage source behind an impedance and the GFM is able to create the grid [10]. Therefore, the converter is capable of controlling the voltage waveform after its filter, in both magnitude and phase, thus controlling active and reactive power and giving support to the grid naturally. To achieve this, a synchronization loop that mimics the behavior of a conventional synchronous generator must be implemented. Several approaches can be found in the literature [6], among them, the so-called Virtual Synchronous Machine (VSM) [11] is one of the most widespread, which replicates the swing equation of a rotating system. Some studies have determined that power systems with large amounts of CBG-based generation must have a significant penetration level of GFM converters in order to be stable [12]. However, a GFM-dominated power system entails some challenges such as low short-circuit ratios, disappearance of physical inertia or resource availability [13]. This points out the importance of studying the stability of largely CBG-penetrated systems.

In this paper, a simulation tool to assess the stability of power systems with a customized generation mix is proposed. The paper proposes modular multi-technology generator model for EMT stability studies, containing the three main kinds of generation topologies: SG, GFL and GFM. The proposed model allows to set the penetration level of each generator technology, being remarkable

useful for stability assessment of power systems with large amounts of CBG. The performance of this block is tested under a fault. Then, this block is used to assess the stability of an equivalent system for different penetration levels of CBG. The employment of EMT simulation is justified when the model involves fast transients, since this simulation technique is capable of calculating in a wide frequency range, from direct current to several kHz. This is the case of power systems that incorporate switching models of CBG, whose dynamics are in the order of tenths of milliseconds.

The paper is structured as follows: Section 2 exhibits and develops the comprehensive models of the generation technologies; Section 3 presents the generator models block and its performance; Section 4 shows the simulation results in an equivalent system designed for testing purposes and Section 5 gathers the conclusions of this work.

2. Generator models

This section describes the topologies that have been considered for the generation technologies studied in this paper, both electrical elements and connections, electronics and control. For this purpose, comprehensive dynamic models have been implemented in the frame of PSCAD/EMTDC software and can be scaled to match the desired penetration level of each technology for EMT studies. A step-up transformer is included at the output of each model.

A. Synchronous generator model

For this model, a non-salient pole synchronous generator has been chosen, representing a conventional large power generator. Regarding the parameters of this model, they have been extracted from the benchmark used by the Spanish TSO [14]. The mechanical model and speed regulator have been implemented following this same proposal. For the exciter model, the standard IEEE ST1A is used. Lastly, a Power System Stabilizer has been implemented as well, following the standard IEEE PSS1A.

B. Grid-following converter model

The model employed for the GFL converter-based generation incorporates a two-level voltage source converter (VSC). A detailed model with the power electronics commutation have been considered in this study. Therefore, an output RL|C filter has been also included to filter the output currents of the converter. The DC voltage is kept constant during the simulations to emulate an ideal generator-side converter controlling this DC voltage, or assuming a large battery is connected to it. The electrical scheme of this model connected to the Thèvenin equivalent of the grid is depicted in Fig. 1. In terms of control strategy, a classical GFL vectorial control scheme has been implemented, including inner current loops and external active/reactive power control loops. In this control strategy, the integration of inner current control loops is given by the need of limiting converter output currents during transient states. The outer control loops are required to deliver/absorb the indicated active and reactive powers, according to the power generation of the plant and the voltage control regulations. Grid synchronization is accomplished through a Phase-Locked Loop (PLL). Fig. 2 illustrates the PLL scheme, while Fig. 3 does for the principal control loops. Model parameters are gathered in TABLE I.

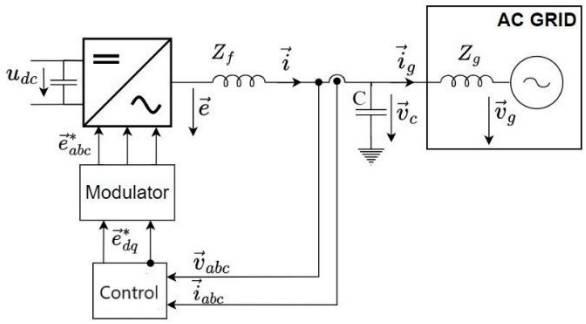

Fig. 1. VSC electrical scheme connected to an equivalent grid model.

TABLE I. Grid-Following converter parameters.

Parameter description	Parameter	Value
Nominal frequency	f_n	50 Hz
Switching frequency	f_{sw}	3 kHz
Filter resistance	R_f	0.03 pu
Filter inductance	L_f	0.2 pu
Filter capacitance	C_f	0.1 pu
Droop constant	R ($K_s = 1/R$)	0.05 pu
(Virtual) Inertia constant	H	2.5 s
Proportional gain PQ regulators	k_{pq}	2
Time constant PQ regulators	T_{ipq}	0.01 s
Proportional gain current regulator	k_p	1.9
Time constant current regulator	T_i	0.1 s
Reactive current module limit	id_{max}	1.15 pu
Active current module limit	iq_{max}	1.15 pu
Damping factor of PLL frequency filter	$\zeta_{filtro\ f_{PLL}}$	0.7
Cut-off frequency of PLL frequency filter	$f_{filtro\ f_{PLL}}$	3 Hz

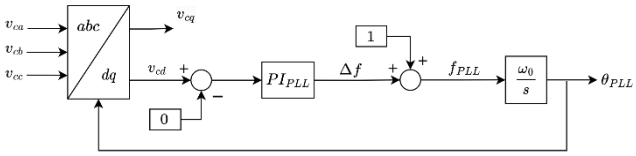

Fig. 2. PLL block diagram.

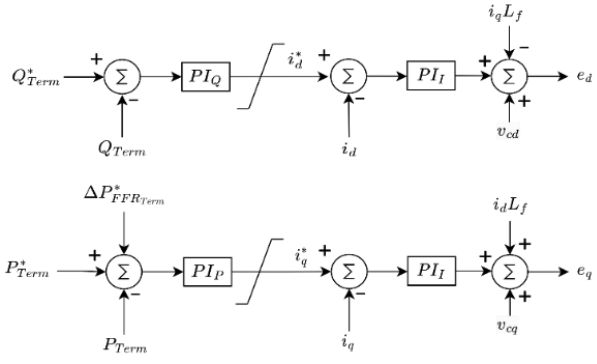

Fig. 3. GFL main control loops block diagram.

As an addition to the main control loops, a well-known frequency support strategy for GFL control, so-called Fast-Frequency Response (FFR) [15] has been included. This control strategy allows the converter to contribute to restore the frequency in conventional systems after a frequency excursion. To achieve this, an active power increment calculated from the PLL measured frequency is added to the total active power reference. This increment includes two terms: an inertial term, based on the Rate of Change of Frequency (ROCOF), calculated by means of a moving average of 500 ms as stablished by the Spanish grid codes [16]; and a proportional term, emulating the droop control of a conventional generator.

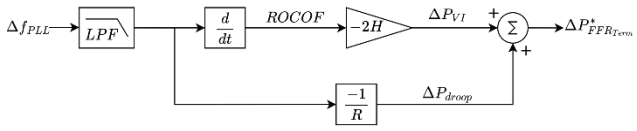

Fig. 4. GFL FFR control loops block diagram.

C. Grid-forming converter model

The GFM converter model follows an identical electrical scheme as the GFL model, see Fig. 1. Therefore, this model only differs on the control strategy. A GFM control technique requires an autonomous synchronization technique, so it can keep itself stable operating in weak grids or even in isolated systems. For this purpose, an active power-based VSM synchronization loop is implemented, given the close relation of the active power with the voltage angle. This loop emulates the swing equation of a rotating system, such as a SG-based system, providing a better approximation to the response of a SG than other approaches, making this model more suitable for operating in a conventional system. The output of this loop is therefore an angle that sets the control angular reference frame, θ. The VSM synchronization loop block diagram is depicted in Fig. 5. Alongside the synchronization loop, two main control loops are implemented. These main control loops are in charge of keeping the converter output voltage (i.e., the capacitor voltage, $\overrightarrow{v_c}$) synchronized. Thus, the synchronous components of this voltage phasor (v_{cd} and v_{cq}) are calculated and oriented to the reference provided by the synchronization loop, θ. To provide a current limitation, which is needed to avoid overcurrents that could damage the converter due to the voltage source behavior acquired with this control, inner control loops are included. Cross-coupling terms have also been implemented to improve the dynamics of these loops. The main control loops are depicted in Fig. 6.

After a grid frequency disturbance, the control reacts as follows: assuming that the voltage synchronous components maintain their synchronization over the disturbance, the damping constant of the synchronization loop, D, provides an active power response proportional to the frequency deviation, similar to the droop speed regulator of a SG but lacking thermal and mechanical dynamics; besides, the inertia constant, H, provides a response proportional to the ROCOF, emulating the inertial response that a SG gives naturally. TABLE II gathers the main parameters of the GFM control. The rest of the parameters are the same as for the GFL converter.

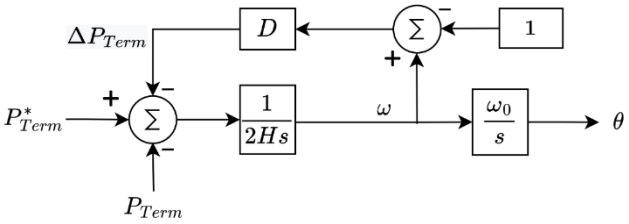

Fig. 5. VSM synchronization loop block diagram.

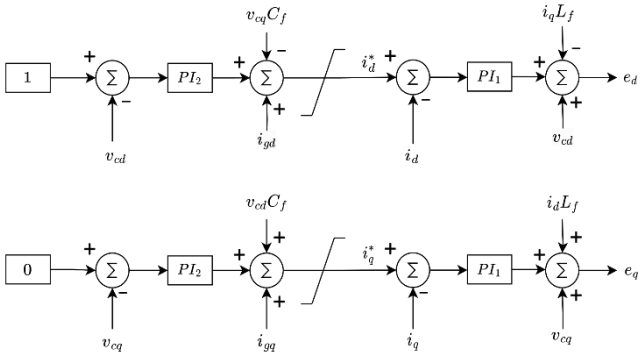

Fig. 6. GFM converter voltage control loops.

TABLE II. Grid-forming converter main parameters.

Parameter description	Parameter	Value
Base angular speed	$\boldsymbol{\omega_0}$	2π50 rad/s
Damping constant	D	100 pu
Virtual inertia constant	H	0.2 s
Voltage regulator proportional gain	k_{pv}	0.39
Votlage regulator time constant	T_{iv}	0.0048 s

3. Proposed modular multi-technology generation model

This paper proposes a new method for simulating power systems with different penetration levels of diverse generation technologies, considering both SG and CBG. This method is based on what has been called modular multi-technology generation model block. This block clusters the three generator models previously described: SG, GFL converter and GFM converter. Fig. 7 shows the electrical scheme of this block when connected to a generic bus of a power system. The penetration level of each generation model (α) are defined as follows:

$$\alpha_{SG} = \frac{S_{SG,N}}{S_{G,N}}, \alpha_{GFM} = \frac{S_{GFM,N}}{S_{G,N}}, \alpha_{GFL} = \frac{S_{GFL,N}}{S_{G,N}} \qquad (1)$$

where and $S_{SG,N}$, $S_{GFM,N}$ and $S_{GFL,N}$ are the nominal apparent power values of the synchronous generation, GFM converter-based generation and GFL converter-based generation, respectively; while $S_{G,N}$ is the nominal apparent power of the total generation connected at the Point Of Connection (POC).

Each generation model considered in this block represents an aggregate model of its generation technology to make scaling easier for simulation purposes. The total output active and reactive power of the block is equal to the sum of the output active and reactive power of each generation model. Each generation model is connected to

the bus through their own step-up transformer modelled as an ideal transformer (no parallel branch considered) with a leakage inductance of 0.15 p.u. The independent voltage/reactive power control is enabled by the inclusion of this transformer, giving an electrical decoupling between each model.

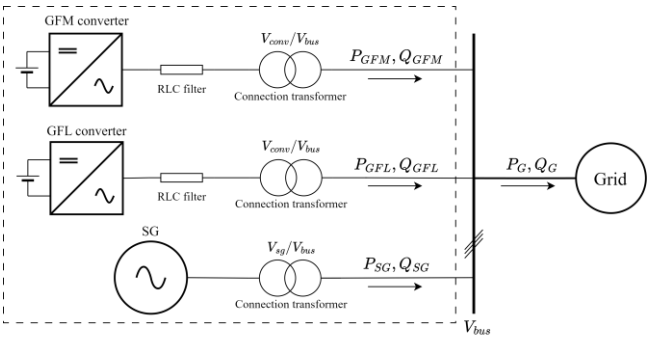

Fig. 7. Model generation block electrical scheme.

Regarding the simulations, the penetration level of each generation technology is directly set through the parameters in the mask of the block, as well as the parameters and the operating conditions of each generator. Note that, in the simulations, the GFL model is working in PQ mode while the SG and GFM converter regulate voltage and frequency.

The main advantages of the proposed multi-technology generation model are that: (a) its implementation and concept are very simple and (b) they can be very useful of stability assessment of power systems with large amounts of CBG, allowing to analyze easily different penetration levels of each generation technology.

A simulation has been carried out to clarify the operation of this block and also to show the different behavior and interactions of each generation technology connected to the same bus and under the same disturbance. For this purpose, the block has been connected to a power source with a short-circuit ratio of 50, representing a strong grid and each technology has a penetration of 1/3 of the total generation of the bus, which is 100 MVA. The chosen disturbance has been a short-circuit of 0.5 depth at the bus. The disturbance occurs at t=6 s. In Fig. 8, the active power response of each technology is depicted. It is shown that SG and GFM generation are injecting more active power during the voltage sag, this due to a higher voltage level behind the connection transformer, which they achieve by injecting a larger amount of reactive power during this transient, as depicted in Fig. 9. However, these two technologies suffer the most when the voltage level is restored. In the case of SG, power oscillations are injected to the grid after the voltage sag, taking several seconds to be damped. On the other hand, the GFM generation transiently loses the synchronization with the grid after the recovery, but fastly resynchronizing, in approximately 400 ms. The GFL generation exhibits less fluctuations during the simulation, being synchronized during the whole process and with a slight overshoot after the voltage recovery; but not providing any voltage support during the transient, aggravating the disturbance. In Fig. 10 the output active and reactive powers of this block are depicted, note that they are the sum of the output power injections of each generator technology.

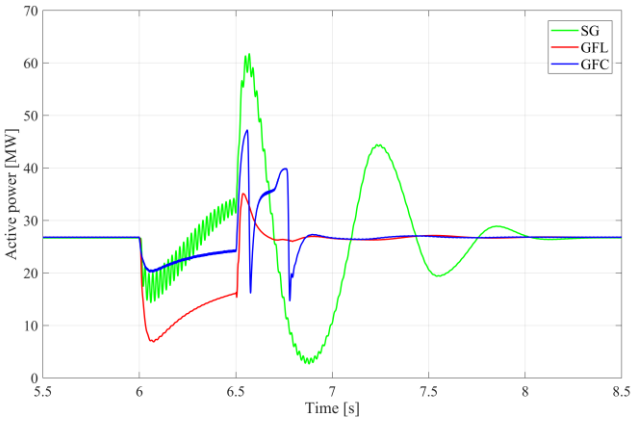

Fig. 8. Active power response of each technology of the generation model block against a short-circuit at the bus.

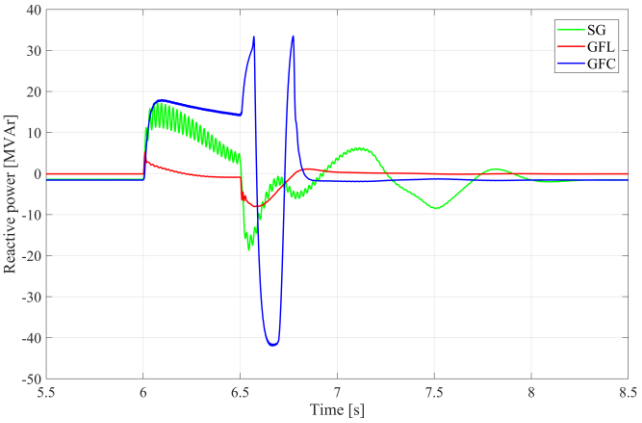

Fig. 9. Reactive power response of each technology of the generation model block against a short-circuit at the bus.

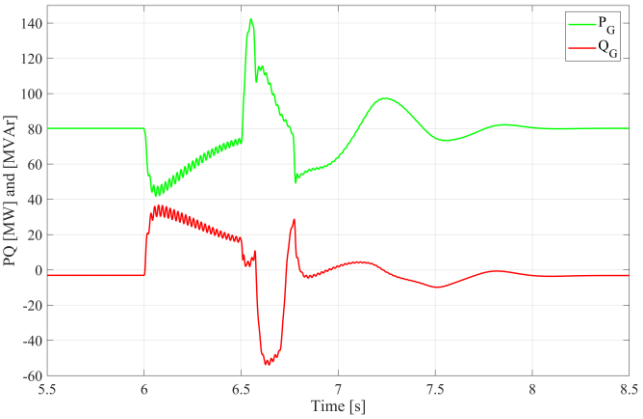

Fig. 10. Total active and reactive power delivered by the generation model block against a short-circuit at the bus.

4. Simulation results in power system

In this section, the stability of two different electrical systems is tested against a certain disturbance for different penetration levels of the proposed generation technologies: SG, GFL converter and GFM converter. For this purpose, the generation model block has been employed and inserted in comprehensive models of electrical systems. EMT simulations have been carried out using PSCAD/EMTDC software for power system stability assessment. These simulations have been carried out in two different electrical system models: the first one based on a small test system.

It should be mentioned that this model has been used successfully also in large-scale EMT studies [17].

A. Two-generator test system

The electrical scheme of this system is depicted in Fig. 11, where the proposed modular generation block model is employed and the grid also contains a synchronous generator, as a representation of the rest of the system. Data used is similar to the benchmark system presented in [14] and gathered in TABLE III and
TABLE IV.

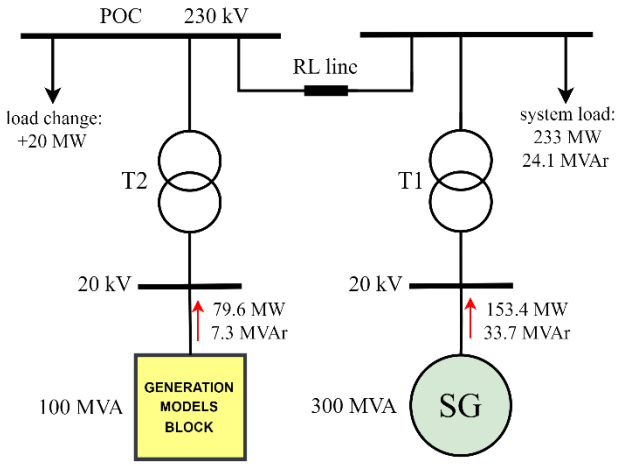

Fig. 11. Test system used.

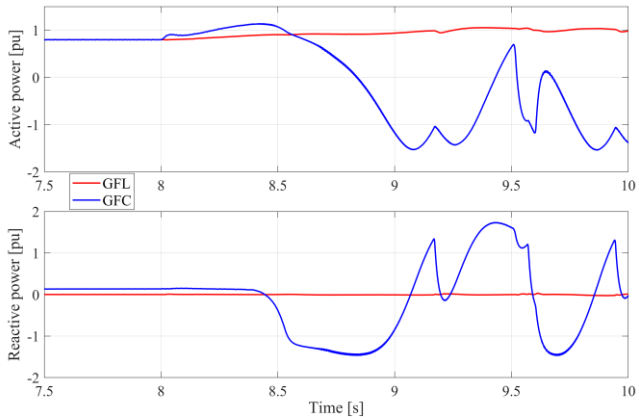

Fig. 12. Active and reactive powers evolution of GFL and GFM generation technologies after a load change at the POC with a penetration of 90 % GFL and 10 % GFM.

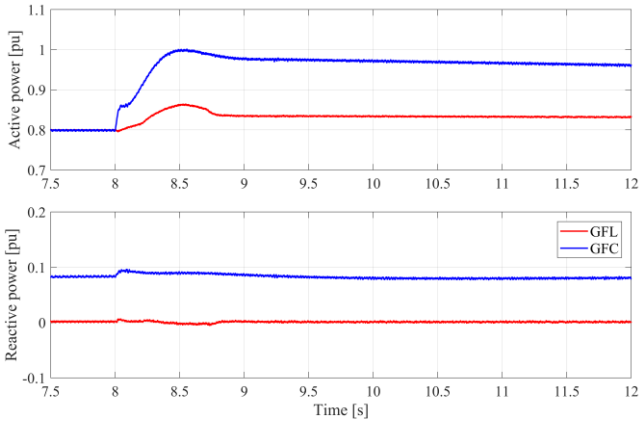

Fig. 13. Active and reactive powers evolution of GFL and GFM generation technologies after a load change at the POC with a penetration of 10 % GFL and 90 % GFM.

In this case, the stability of the system is studied for a given level of CBG-only penetration in the generation model block, given that the rest of the generation is modelled as a SG. In particular, the differences in the response of each technology for both cases are observed. In order to test the stability of the system under small disturbances, a sudden load change of 20 MW (0.05 pu) is applied at the local load (POC) at t=8 s. Two cases are compared:

- Case 1: $\alpha_{GFM} = 10\ \%$ and $\alpha_{GFL} = 90\ \%$.
- Case 2: $\alpha_{GFM} = 90\ \%$ and $\alpha_{GFL} = 10\ \%$.

In the first case, $\alpha_{GFM} = 10\ \%$ and therefore $\alpha_{GFL} = 90\ \%$. The active and reactive power responses of GFM and GFL generation are depicted in Fig. 12. It can be observed that the low penetration level of GFM generation leads towards a loss of synchronism by this kind of generation after the load change, even with a frequency support strategy implemented on the GFL generation. For the second case, $\alpha_{GFM} = 90\ \%$ and $\alpha_{GFL} = 10\ \%$. The active and reactive power responses are depicted in Fig. 13. In this case, the simulation is stable after the disturbance. Attending to the active power response, the GFM generation is providing both inertial and frequency support from the first instants after the load change and the GFL generation is emulating both frequency responses by means of its FFR strategy, with a certain response delay. Regarding the reactive power, the GFM is in charge of the bus voltage control, and therefore the amount of reactive power injected by this technology increases after the disturbance; on the other hand, the GFL generation is working in PQ mode, so the amount of reactive power injected remains unaltered.

Results show that in power systems with large amounts of CBG, high penetration of GFL generation can lead to instabilities, whilst high penetration of GFM generation could guarantee the stability of the system.

TABLE III. Line and transformers parameters of the two-generator test system.

Parameter description	Parameter	Value
T1: Rated power	S_N	300 MVA
T1: Rated line-line voltage primary	V_{1N}	230 kV
T1: Rated line-line voltage secondary	V_{2N}	20 kV
T1: Short-circuit ratio	Z_{sc}	12 %
T1: X/R ratio	X/R	30 pu
T1: Rated frequency	f	50 Hz
T2: Rated power	S_N	100 MVA
T2: Rated line-line voltage primary	V_{1N}	230 kV
T2: Rated line-line voltage secondary	V_{2N}	20 kV
T2: Short-circuit ratio	Z_{sc}	10 %
T2: X/R ratio	X/R	25 pu
T2: Rated frequency	f	50 Hz
LINE: Inductance	L_l	2.8 mH
LINE: Resistance	R_l	0.29 Ω

TABLE IV. Synchronous generator parameters of the two-generator test system.

Parameter description	Parameter	Value
Rated power	S_N	200 MVA
Rated line-line voltage	V_N	5 kV
Frequency	f_s	50 Hz
Poles pair number	p	2
Stator winding resistance	R_s	0.02 pu
Stator leakage inductance	L_s	0.112 pu
d-axis magnetizing inductance	L_{dm}	1.79 pu
q-axis magnetizing inductance	L_{qm}	1.6 pu
Field winding resistance (referred to stator)	R_f	1.21 pu
Field winding leakage inductance (referred to stator)	L_{fl}	0.117 pu
Rotor damping cage d-axis resistance (referred to stator)	R_{dr}	0.03 pu
Rotor damping cage d-axis leakage inductance (referred to stator)	L_{drl}	0.375 pu
Rotor damping cage q-axis resistance (referred to stator)	R_{qr}	0.004 pu
Rotor damping cage d-axis leakage inductance (referred to stator)	L_{qrl}	0.2 pu
Inertia constant	H	2.5 s
Stator and rotor windings turn ratio	N_s/N_r	1/3

5. Conclusion

In this paper, a modular multi-technology generator model for EMT stability studies in power systems with large amounts of CBG has been proposed. The conclusions obtained from this work are as follows:

- The implementation and concept of the proposed modular multi-technology generator model are very simple.
- The proposed modular multi-technology generator model can be very useful of stability assessment of power systems with large amounts of CBG, allowing to analyze easily different penetration levels of each generation technology.
- Simulation results illustrate the need of certain amount of GFM generators in power system with large amounts of CBG to guarantee power system stability.

Acknowledgements

The results presented in this paper are part of a R&D project with reference: K-ER53-IDGFC, which is a collaboration between Universidad Carlos III de Madrid, CITCEA-UPC and Red Eléctrica-Redeia. The project was funded by Red Eléctrica-Redeia.

References

[1] IRENA, "Renewable Capacity Statistics 2023," 2023. [Online]. Available: www. irena.org

[2] IRENA, *Grid codes for renewable powered systems.* 2022. [Online]. Available: www.irena.org/publications

[3] Y. Cheng, R. Azizipanah-Abarghooee, S. Azizi, L. Ding, and V. Terzija, "Smart frequency control in low inertia energy systems based on frequency response techniques: A review," *Appl. Energy*, vol. 279, no. March, p. 115798, 2020, doi: 10.1016/j.apenergy.2020.115798.

[4] R. Rosso, X. Wang, M. Liserre, X. Lu, and S. Engelken, "Grid-forming converters: An overview of control approaches and future trends," *ECCE 2020 - IEEE Energy Convers. Congr. Expo.*, pp. 4292–4299, 2020, doi: 10.1109/ECCE44975.2020.9236211.

[5] W. Du *et al.*, "Modeling of Grid-Forming and Grid-Following Inverters for Dynamic Simulation of Large-Scale Distribution Systems," *IEEE Trans. Power Deliv.*, vol. 36, no. 4, pp. 2035–2045, 2021, doi: 10.1109/TPWRD.2020.3018647.

[6] D. B. Rathnayake *et al.*, "Grid Forming Inverter Modeling, Control, and Applications," *IEEE Access*, vol. 9, pp. 114781–114807, 2021, doi: 10.1109/ACCESS.2021.3104617.

[7] National Grid, "Perform of Phase-Locked Loop Based Converters," *System Operability Framework*, 2017.

[8] X. Meng, J. Liu, and Z. Liu, "A Generalized Droop Control for Grid-Supporting Inverter Based on Comparison between Traditional Droop Control and Virtual Synchronous Generator Control," *IEEE Trans. Power Electron.*, vol. 34, no. 6, pp. 5416–5438, 2019, doi: 10.1109/TPEL.2018.2868722.

[9] Energy Systems Integration Group (ESIG), "Grid-Forming Technology in Energy Systems Integration," 2022.

[10] A. Dyśko *et al.*, "Testing characteristics of grid forming converters part I : Specification and Definition of Behaviour," *19th Wind Integr. Work.*, no. April 2021, 2020, [Online]. Available: https://strathprints.strath.ac.uk/74726/

[11] H. P. Beck and R. Hesse, "Virtual synchronous machine," *2007 9th Int. Conf. Electr. Power Qual. Util. EPQU*, pp. 7–12, 2007, doi: 10.1109/EPQU.2007.4424220.

[12] B. J. Matevosyan, H. Urdal, S. Achilles, J. Macdowell, J. O. Sullivan, and R. Quint, "Grid-Forming Inverters," no. October, pp. 89–98, 2019.

[13] ENTSO-E, "System dynamic and operational challenges," no. November, 2021, [Online]. Available: https://tyndp.entsoe.eu/news/2020/08/93-gw-of-additional-solutions-for-cross-border-electricity-exchange-needed-by-2040-to-achieve-the-eu-green-deal/

[14] "Norma técnica de supervisión de la conformidad de los módulos de generación de electricidad según el Reglamento UE 2016/631." p. 200, 2021. [Online]. Available: https://api.esios.ree.es/documents/642/download?locale=es

[15] ENTSO-E, "High Penetration of Power Electronic Interfaced Power Sources and the Potential Contribution of Grid Forming Converters," p. 32, 2019, [Online]. Available: https://www.entsoe.eu/Documents/Publications/SOC/High_Penetration_of_Power_Electronic_Interfaced_Power_Sources_and_the_Potential_Contribution_of_Grid_Forming_Converters.pdf

[16] BOE, "Orden TED/749/2020, de 16 de julio, por la que se establecen los requisitos técnicos para la conexión a la red necesarios para la implementación de los códigos de red de conexión," *Boletín Of. del Estado*, no. 11, pp. 2260–2268, 2019, [Online]. Available: https://www.boe.es/boe/dias/2019/01/12/pdfs/BOE-A-2019-317.pdf

[17] J. C. Martínez *et al.*, "Stability Assessment in Power Systems with High Penetration of Converter-based Generation," in *2023 IEEE International Conference on Environment and Electrical Engineering and 2023 IEEE Industrial and Commercial Power Systems Europe (EEEIC / I&CPS Europe)*, Jun. 2023, pp. 1–6. doi: 10.1109/EEEIC/ICPSEurope57605.2023.10194891.